A MODEL FOR AN ANISOTROPIC ELASTIC STATE

V. M. Zhigalkin and G. L. Lindin

UDC 539.374

A plastic-strain mechanism has been suggested [1, 2] which involves intermediate slip areas [3]. This mechanism provides work-hardening equations for any form of loading in which the principal directions in the stress tensor are unchanged, and it is sufficient for the purpose to know the work-hardening law for axial tension.

Here we report experiments in which loading of biaxial tension type has been used with tubular specimens of 40Kh steel subject to internal pressure and axial forces. The principal directions in the stress tensor remain at rest within the body, although the loading is substantially different from proportional.

§1. Consider the state of stress in an element having immobile principal directions for the stress tensor (1-3) in Fig. 1; let the inequalities

$$\sigma_1 \geqslant \sigma_2 \geqslant \sigma_3 \tag{1.1}$$

be met without reenumeration; the origin of the auxiliary coordinate system (n_1, n_2, n_3) is located on the surface of unit sphere described around the element. The slip area τ_{31} is the area having normal n_3 and direction n_1 in it. The tangential stress τ'_{31} on this area (α, β, φ) takes the following form (Fig. 1):

$$\tau'_{31} = \frac{\sigma_1}{2}\cos\beta\cdot\sin 2\varphi + \frac{\sigma_2}{2}(\sin 2\alpha\,\sin\beta\cdot\cos\varphi - \sin^2\alpha\cdot\cos\beta\cdot\sin 2\varphi) -$$

$$-\frac{\sigma_3}{2}(\sin 2\alpha\cdot\sin\beta\cdot\cos\varphi + \cos^2\alpha\cdot\cos\beta\ \sin 2\varphi).$$

The principal slip areas $T = (\sigma_1 - \sigma_3)/2$, $T_{12} = (\sigma_1 - \sigma_2)/2$, $T_{23} = (\sigma_2 - \sigma_3)/2$ are accompanied by the following intermediate areas [3]:

$$\beta = 0;\ \varphi = \pi/4;\ \alpha = \pm\pi/4,\ \alpha = \pm 3\pi/4, \tag{1.2}$$

on which there is the tangential stress $T'_{12} = (T + T_{12})/2$; if axes 1 and 3 are interchanged in Fig. 1, the slip areas of (1.2) are subject to the tangential stress $-T'_{23}$, where $2T'_{23} = T + T_{23}$, and it is clear that

$$T_{12} \leqslant T'_{12},\ T_{23} \leqslant T'_{23}.$$

If axes 1 and 2 are interchanged, we get the tangential stress $T'_{21} = (T_{23} - T_{12})/2$ on the slip areas of (1.2).

A deformation mechanism has been described [3] in which the plastic strain is represented as a sequence of shears on the slip areas T, T_{12}, T_{23} [1, 2] and T'_{12}, T'_{23}, T'_{21}; the sides of the regular hexagons in the deviator plane in Fig. 2a relate to the lines $T_{ij} \equiv \text{const} = \tau_L$ ($i < j$), where τ_L is the yield point in shear. Condition (1.1) defines region A, in which τ_L is attained only on the slip areas T, T_{12}, T_{23}, T'_{12}, T'_{23} in response to actual loads. For this area we adopt assumption I on the independence of the T, T_{12}, T_{23}, T'_{12}, T'_{23} slip areas: the total plastic shear γ on the slip areas corresponding to a given tangential stress is dependent only on the maximum value:

$$\gamma_{ij} = F(T_{ij}),\ \gamma'_{ij} = F(T'_{ij}), \tag{1.3}$$

where F is the standard relationship for the material. This allows us to sum the contributions from the different areas to the plastic strain, for the work of plastic strain A^P done by the tangential stresses T, T_{12}, T_{23}, T'_{12}, T'_{23} is given by (1.3) as having the increment

Novosibirsk. Translated from Zhurnal Prikladnoi Mekhaniki i Tekhnicheskoi Fiziki, No. 1, pp. 161-166, January-February, 1977. Original article submitted March 22, 1976.

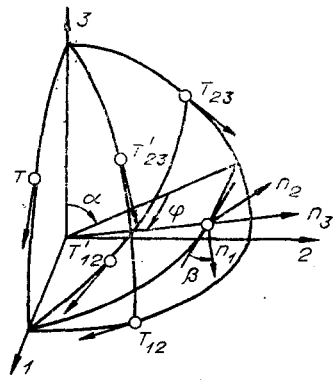

Fig. 1

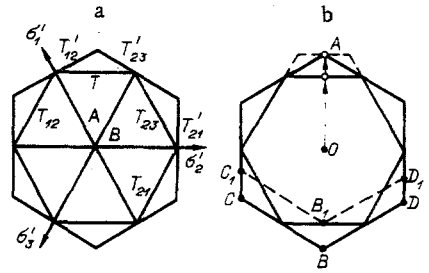

Fig. 2

$$\Delta A^p = TF'(T)\Delta T + T_{12}F'(T_{12})\Delta T_{12} + \ldots + T'_{23}F'(T'_{23})\Delta T'_{23}, \tag{1.4}$$

where $F'(T_{ij}) = dF(T_{ij})/dT_{ij}$; if the variable T_{ij}, and T'_{ij} are the maximum attainable values (not the current values of the tangential stresses), they are not dependent, and the value of ΔA^p in the form of (1.4) is the total differential in terms of these variables, while A^p itself is not dependent on the mode of loading on passing from one state of strain to another. To calculate A^p we used a stepwise loading path in (1.4), in which the slip areas were successively activated. The increments in the plastic strains $\Delta\varepsilon^p_\alpha$ (α = 1, 2, 3) were derived as the corresponding coefficients to σ_α in (1.4):

$$\begin{aligned}\Delta A^p = \sigma_1\left[\frac{F'(T)}{2}\Delta T + \frac{F'(T_{12})}{2}\Delta T_{12} + \frac{F'(T'_{12})}{2}\Delta T'_{12} + \frac{F'(T'_{23})}{4}\Delta T'_{23}\right] + \\ + \sigma_2\left[\frac{F'(T_{23})}{2}\Delta T_{23} - \frac{F'(T_{12})}{2}\Delta T_{12} - \frac{F'(T'_{12})}{4}\Delta T'_{12} + \frac{F'(T'_{23})}{4}\Delta T'_{23}\right] - \\ - \sigma_3\left[\frac{F'(T)}{2}\Delta T + \frac{F'(T_{23})}{2}\Delta T_{23} + \frac{F'(T'_{12})}{4}\Delta T'_{12} + \frac{F'(T'_{23})}{2}\Delta T'_{23}\right],\end{aligned} \tag{1.5}$$

which shows that the contributions from the slip areas add up.

In order to determine F(T) it is sufficient to know the work-hardening law ε^p_1 (σ_1) for axial stretching; in fact, we have $T \equiv T_{12} \equiv T'_{12}$, $T'_{23} \leq \tau_L$, $T_{23} = 0$ for this form of loading, so (1.5) gives us

$$\Delta\varepsilon^p_1(T) = \frac{3\Delta T}{2}F'(T),$$

whence we get

$$F(T) = \frac{2}{3}\varepsilon^p_1(T). \tag{1.6}$$

We now consider loading with immobile principal directions for the stress tensor but with the restrictions of (1.1) eliminated; then plastic shear can occur on six slip areas (or 12 areas in Fig. 2a if the sign of the tangential stress is incorporated). In that case, we make assumption II, which governs the slip areas: the slip areas $\pm T_{ij}$ are not dependent in the sense of (1.3), while hardening on one such area may cause various degrees of softening on the slip areas T'_{qp} related to two sides of the external hexagon opposite the given side. Figure 2b shows the projection of the loading surface on the deviator plane for loading path OA. Hardening on slip area T causes softening on the areas related to sides BC and BD. The new sides B_1C_1, and B_1D_1 correspond to the tangential stress τ_{L_1}:

$$\tau_{L1} = \tau_L - (T^0 - \tau_L), \tag{1.7}$$

where T^0 is the maximum value of T.

Assumption II resembles assumption I in allowing us to sum the contributions from the various slip areas to the plastic strain.

We now consider how the slip areas vary when the loading path goes from region A to region B in Fig. 2a; in the latter case, $\sigma_2 > \sigma_1 > \sigma_3$, because the slip areas $T_{21} = (\sigma_2 - \sigma_1)/2$, $T'_{21} = (T_{23} + T_{21})/2$ are activated. If $T_{12} > \tau_L$ in region A, then (1.7) indicates that the additional contributions to the increment in the plastic strain are

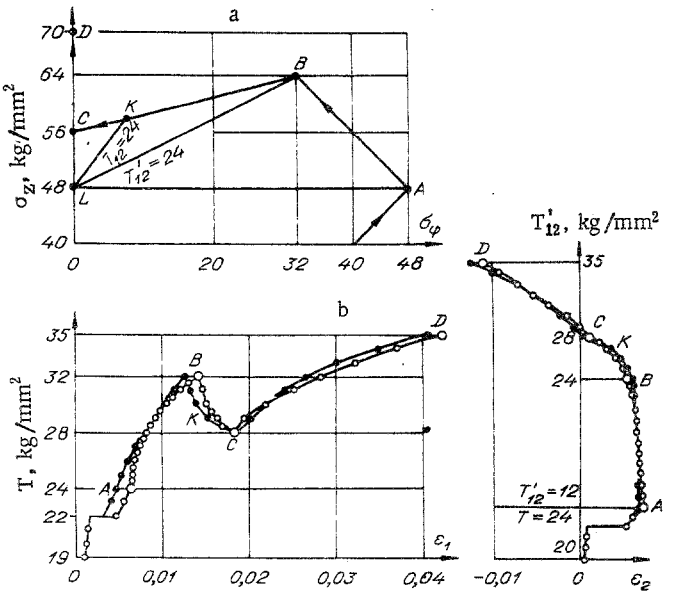

Fig. 3

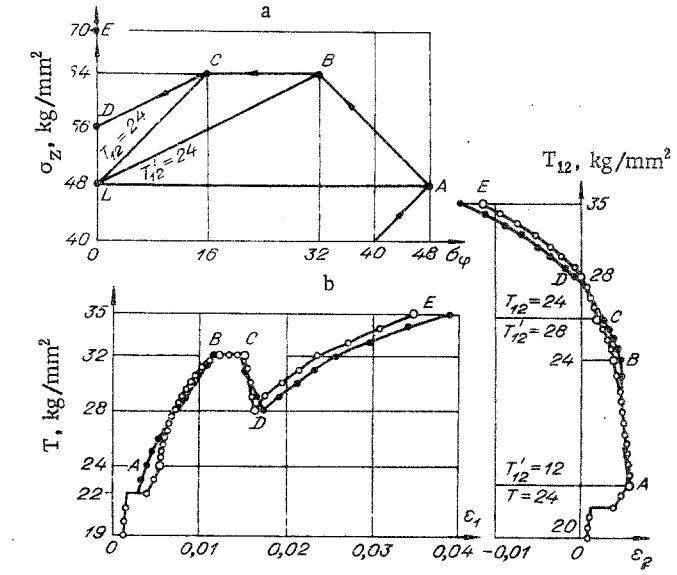

Fig. 4

$$\Delta\varepsilon_1^p:-\frac{F'(T_{21})}{2}\Delta T_{21}-\frac{F'\left(T'_{21}+T_{12}-\tau_L\right)}{4}\Delta T'_{21},$$

$$\Delta\varepsilon_2^p:\frac{F'(T_{21})}{2}\Delta T_{21}+\frac{F'\left(T'_{21}+T_{12}-\tau_L\right)}{2}\Delta T'_{21}, \qquad (1.8)$$

$$\Delta\varepsilon_3^p:-\frac{F'\left(T'_{21}+T_{12}-\tau_L\right)}{4}\Delta T'_{21}.$$

If $T_{21} > \tau_L$ in region B, then we have to replace $F'(T'_{12})$ by $F'(T'_{12}+T_{21}-\tau_L)$ in (1.5) on returning to region A, where T_{21} and T_{12} in (1.8) are the maximum attainable values for the corresponding tangential stresses.

Figure 2b illustrates the behavior of (1.5) and (1.8) by means of loading surfaces, and it is clear that these equations describe the combined hardening involving coupled planar loading surfaces [4].

§2. We now compare these results with experiments in which the loading was of biaxial tension type in thin-walled tubes made of 40Kh steel subject to internal pressure and axial forces.

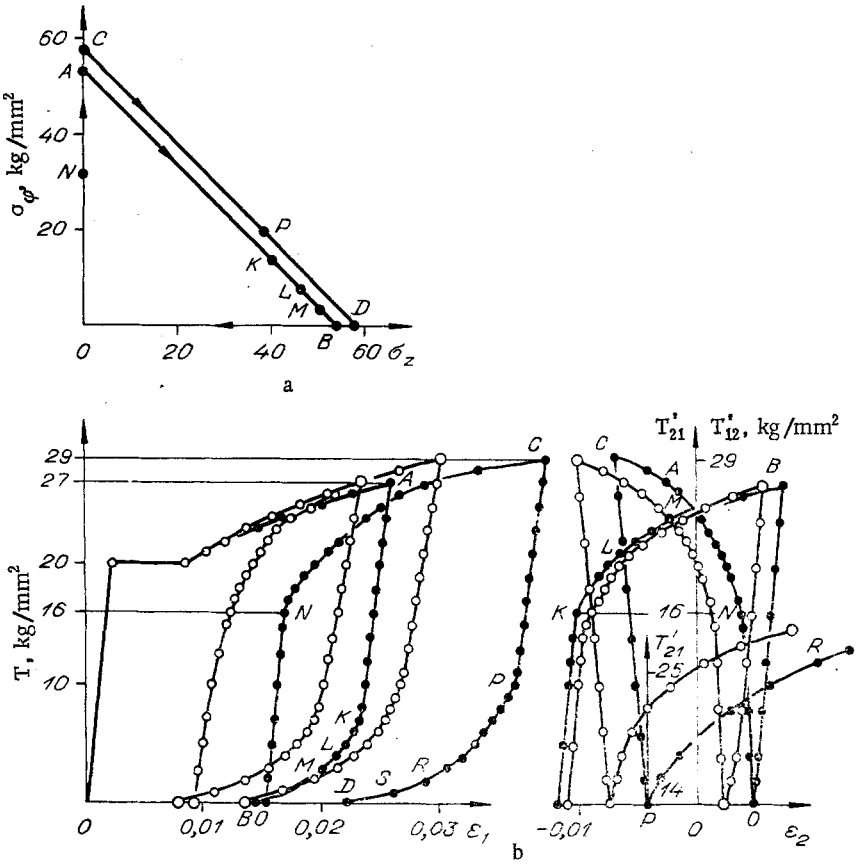

Fig. 5

The specimens were hollow cylinders of wall thickness δ = 1 mm in the working part and average radius R = 15 mm; the differences in wall thickness did not exceed ±0.01 mm. The specimens were heat treated at 800°C and 10^{-4} mm Hg for 2.5 h; this was sufficient to produce a definite yield range.

The strain was measured with strain gauges and dial gauges, the latter being used for the longitudinal strain over a baseline of 100 mm, the dial gauge having a scale division of 0.01 mm, while devices of micron sensitivity were used for the transverse strain. The radial strain was deduced from the volume change calculated from Hooke's law. The radial stress was taken as zero. The effects of creep were eliminated by making the measurement at each stage in the strain after a delay of 5 min.

Figures 3-5 show the measurements (open circles) and the calculations (filled circles). These specimens had initial anisotropy: $\sigma_z \neq 0$, τ_{L_1} = 23 kg/mm² in axial tension, $\sigma_\varphi \neq 0$, τ_{L_2} = 20 kg/mm² in circumferential tension, and $\sigma_z \equiv \sigma_\varphi \neq 0$, τ_{L_3} = 22 kg/mm² in uniform biaxial tension. The calculations shown in Fig. 3b and Fig. 4b were based on τ_L = 23 kg/mm² for the slip areas T, T_{12}, T'_{12}, T'_{23} and τ_L = 20 kf/mm² for the slip areas T_{23}, T_{21}, T'_{21} (the values for τ_L on the slip areas are interchanged for the calculation of Fig. 5b).

The F(T) defined from (1.6) for the axial-tension experiments is given for integer T in Table 1.

The calculations were performed as follows. At each stage of loading, starting from the yield range, we calculated T_{ij} and T'_{ij}, which were compared with τ_L and τ_{L_1} in the form of (1.7). As each slip area was activated, we calculated the increments in the plastic strains in accordance with (1.5) and (1.8), where the term $F'(T_{ij})\Delta T_{ij}$ was replaced by $F(T_{ij} + \Delta T_{ij}) - F(T_{ij})$, while the values for F for noninteger T_{ij} were determined from the adjacent integer values by interpolation. This calculation is conveniently performed by computer.

Figures 3a and 4a show the loading paths ABCD and ABCDE in region A: up to point A, there is uniform biaxial extension, while on part AB only one slip area T is active, i.e., $T > \tau_L$ and $\Delta T > 0$, so (1.5) indicates elastic variation in ε_2, i.e., $\Delta\varepsilon_2^p = 0$.

TABLE 1

T, kg/mm²	$F(T)\cdot 10^3$	T, kg/mm²	$F(T)\cdot 10^3$	T, kg/mm²
23	0	29	2,31	35
24	0,25	30	2,81	36
25	0,58	31	3,34	37
26	0,96	32	3,98	38
27	1,38	33	4,77	—
28	1,83	34	5,76	—

Here we should note that the component of the stress deviator $\sigma_2' = \sigma_1' > 0$ at point A, so Mises' theory indicates that there is plastic change in ε_2 (with $\Delta\varepsilon_2^p > 0$), which conflicts with experiment.

Figure 5a shows the loading path OABOCD as emerging from region A and passing to region B and vice versa. The softening on the slip areas T_{21}' and T_{12}' was examined in terms of T_{21} plotted on the right in Fig. 5b, for the loading sections ABO and PD, and also the value of T_{12}' for the loading section OCP, the relevant point here being which slip area was activated (the elastic changes in ε_1 and ε_2 cease when these areas are activated). We see from (1.5) and (1.8) that slip area T_{21}' is activated at 16 kg/mm² (point K) in the first cycle and at 14 kg/mm² (point P) in the second one. Similarly, area T_{12}' is activated at 16 kg/mm² (point N).

Therefore, Figs. 3-5 show satisfactory agreement between the calculations and experiment on loading with immobile principal directions for the stress tensor.

We are indebted to E. I. Shemyakin for valuable comments.

LITERATURE CITED

1. E. I. Shemyakin,"Anisotropy in the plastic state," in: Numerical Methods in the Mechanics of Continuous Media [in Russian], Izd. Vychisl. Tsentr Sibirsk. Otd. Akad. Nauk SSSR, Vol. 4, No. 4 (1973).
2. S. A. Khristianovich, "Strain in a work-hardening plastic material," Izv. Akad. Nauk SSSR, Mekh. Tverd. Tela, No. 2 (1974).
3. G. L. Lindin, "Work hardening in an elastoplastic body," Zh. Prikl. Mekh. Tekh. Fiz., No. 3 (1976).
4. I. V. Knets, The Major Current Trends in the Mathematical Theory of Plasticity [in Russian], Zinatne, Riga (1971), p. 39.